Measuring Droplets Expelled During Endoscopy to Investigate COVID-19 Transmission Risk

Severe acute respiratory syndrome coronavirus-2 (SARS-CoV-2) infection spreads primarily through droplets and aerosols.[1] Various procedures in health care, including upper endoscopy, have been categorized as aerosol-generating procedures.[2] However, whether these procedures also produce significant quantities of larger droplets, which pose a greater transmission risk, is unclear.[3] It is also unclear whether colonoscopies cause an additional risk for health care workers, because fecal-oral transmission has been identified as a possible transmission mechanism.[2]

The ability to detect and measure droplets is critical for the evaluation of procedure risk, but most available methods lack portability or cannot distinguish solid particles from liquid droplets, which pose a much higher risk of SARS-CoV-2 transmission.[1] To investigate the droplet-generating risk posed by endoscopy procedures, we developed a robust and portable optical instrument capable of distinguishing liquid droplets from solid particles while also measuring the size and quantity of fast-flying droplets in the clinical setting.

The system was designed to image the angular dependent light-scattering patterns produced by droplets in the close to forward direction. Mie theory[4] shows that this scattering pattern can be exploited to determine droplet size.[5] The optical layout of the system is shown in Figure 1A and B. Droplets cross an expanded red laser beam after entering through an aperture in the 3D printed case (Figure 1C). One camera images the angular dependent light-scattering patterns, while a second camera is used to spatially visualize the droplets and co-register them with their scattering patterns. The larger fan maintains an air flow, while the smaller fan cools the cameras. The entire system was constructed on an 8- × 10-inch optical breadboard and provides a measurement zone of 5 × 12 mm.

The system was used to measure droplets produced during 10 upper endoscopies and 10 colonoscopies. The study was performed according to the Beth Israel Deaconess Medical Center Institutional Review Board guidance.

Consecutive procedures were measured in a single room over 2 days. Measurements were taken during 3 time periods for each patient, with 1 period corresponding to the procedure duration and the other 2 periods corresponding to controls. During the preprocedure control, the patient and staff were present in the procedure room, but the endoscope had not been inserted into the patient. For the postprocedure control, the endoscope had been removed from the patient, but both staff and patient were still present. The positioning of the device for the upper endoscopy procedures is illustrated in Figure 1D and E. Measurements were taken near the rectum for colonoscopy procedures. Best estimates for the device positioning are given in Supplementary Table 1.

The data were analyzed by initially extracting the scattering events that occurred during the procedure and controls. A scattering event occurs when a liquid droplet or solid particle crosses the beam, with typical scattering patterns for each type shown in Figure 1F and G, respectively. Figure 1H shows the average number of scattering events per unit area per minute for all procedures and controls. Figure 1I shows the results when only droplets were considered, while Figure 1J and K shows the droplet size distribution for upper endoscopies and colonoscopies, respectively. Most detected droplets had diameters between 40 μm and 50 μm.

The number of scattering events, which includes droplets and particles, was considerably higher for both controls compared with the procedures. This was not unexpected, because there is much more activity in the procedure room before and after the procedure. However, significantly more droplets that pose a transmission risk were observed in the procedures compared with the controls. More droplets were measured during colonoscopy procedures compared with upper endoscopy procedures ($4.0 \cdot 10^{-2}$ mm^{-2} and $2.8 \cdot 10^{-2}$ mm^{-2}, respectively). When adjusted for procedure duration, more droplets per unit time were produced during the upper endoscopies than during the colonoscopies ($3.6 \cdot 10^{-3}$ mm$^{-2} \cdot$ min^{-1} and $1.9 \cdot 10^{-3}$ mm$^{-2} \cdot$ min^{-1}, respectively). However, neither of these differences was statistically significant. A similar size distribution was seen for both procedures, with a slightly larger spread observed for the colonoscopy procedures.

It is possible to estimate the total number of droplets produced during upper endoscopies using spreading angles obtained from cough studies.[6] Given the average measurement distance, we determined that approximately 500 liquid droplets could be produced during upper endoscopy. By converting the droplets to volume and using the average viral load observed by Wölfel et al,[7] it is possible that upper endoscopy procedures produce approximately 6500 viral copies per procedure.

Our results have several important clinical implications. First, the positioning of our device shows that these droplets can reach nearby health care workers.

Second, while the risk of COVID-19 transmission during upper endoscopy has been well recognized, our findings suggest that transmission via droplets during colonoscopy is also possible.

Third, we found marked variation among droplets produced by patients, with 1 patient from the colonoscopy group and 1 patient from the upper endoscopy group accounting for
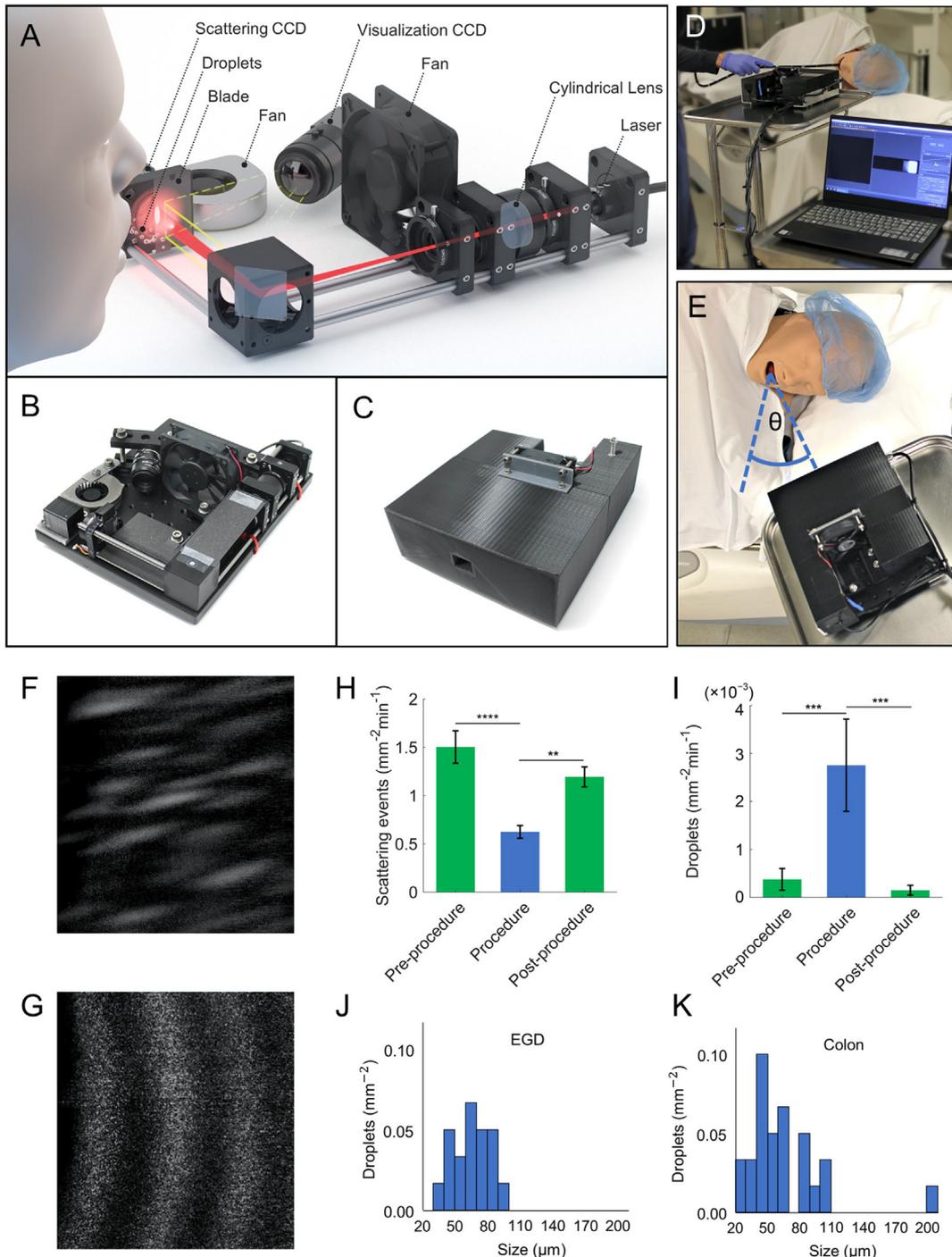
Figure 1. (A) Three-dimensional schematic of the clinical light-scattering system for detecting and sizing expelled droplets shows the illumination, droplet, and visualization paths for preclinical measurements. Head position was rotated by 90° and further from the device for clinical measurements. CCD, charge-coupled device. Photo shows the system (B) without the case and (C) with the 3D printed case. (D) Positioning of system for upper endoscopy procedures. The desired position was as close as possible to the patient's mouth or rectum, with an angular orientation as close as possible to the oral axis or anal canal axis. (E) Illustration of angular notation for system positioning. Device is located approximately 30 cm from the mannequin, with an angle of approximately 30°. Typical scattering pattern produced by (F) a solid particle and (G) a liquid droplet. (H) Scattering events due to both particles and droplets for each interval. The *bar heights* represent the mean values for each category, and the *error bars* represent standard errors. The results are based on 20 clinical endoscopy procedures (10 upper endoscopies and 10 colonoscopies). P value was determined by 1-way analysis of variance, followed by Dunnett's multiple comparisons test. ****$P < .0001$ (procedure vs preprocedure), **$P = .0028$ (procedure vs postprocedure). (I) Droplet only measurements for each interval. P value was determined by the Kruskal-Wallis test, followed by Dunnett's multiple comparisons test. ***$P = .0006$ (procedure vs preprocedure), ***$P = .0001$ (procedure vs postprocedure). The size distribution of droplets produced during (J) upper endoscopy and (K) colonoscopy.

approximately 50% of the total droplets produced. This upper endoscopy patient was not wearing a procedural oxygen mask, but 6 patients were. On average, the unmasked patients produced 2.75-times more droplets than the masked patients. Given that the procedural oxygen mask almost certainly reduces the emission cone, this difference is probably even more significant. We also observed low numbers of droplets for some patients in both the masked and unmasked group, similar to other studies.[8] For the colonoscopy patient that produced the most droplets, the droplets were spread throughout the procedure. Conversely, for the upper endoscopy patient, all droplets came in a single 33-second period and did not correspond to coughing or endoscope insertion/removal. Although other endoscope manipulations may have caused the increased expulsion, it appears that the periods of higher risk may be difficult to identify. To minimize droplet exposure, we suggest only essential personnel remain close to the endoscope operator during the procedure.

To our knowledge, this is the first measurement of large droplets, which pose the biggest transmission risk, in the clinical setting. Our results are not only relevant for SARS-CoV-2, but could also apply to other respiratory viruses, such as influenza.

Supplementary Material

Note: To access the supplementary material accompanying this article, visit the online version of *Gastroenterology* at www.gastrojournal.org, and at https://doi.org/10.1053/j.gastro.2021.07.013

MARK F. COUGHLAN[*]
Center for Advanced Biomedical Imaging and Photonics
Division of Gastroenterology
Department of Medicine
Beth Israel Deaconess Medical Center
Harvard Medical School
Boston, Massachusetts

MANDEEP S. SAWHNEY[*§]
DOUGLAS K. PLESKOW
Center for Advanced Endoscopy
Division of Gastroenterology
Department of Medicine
Beth Israel Deaconess Medical Center
Harvard Medical School
Boston, Massachusetts

CONOR J. SHEIL
Center for Advanced Biomedical Imaging and Photonics
Division of Gastroenterology
Department of Medicine
Beth Israel Deaconess Medical Center
Harvard Medical School
Boston, Massachusetts
GI LIGHT SCATTERING GROUP

LE QIU[§]
LEV T. PERELMAN[§]
Center for Advanced Biomedical Imaging and Photonics
Division of Gastroenterology
Department of Medicine
Beth Israel Deaconess Medical Center
Harvard Medical School
Boston, Massachusetts

References

1. Anfinrud P, et al. N Engl J Med 2020;382:2061–2063.
2. **Sultan S, Lim JK**, et al. Gastroenterology 2020; 159:739–758.
3. Stadnytskyi V, et al. Proc Natl Acad Sci U S A 2020; 117:11875–11877.
4. Mie G. Ann Phys 1908;330:377–445.
5. Glover AR, et al. Appl Opt 1995;34:8409–8421.
6. Tang JW. J R Soc Interface 2009;6:S727–S736.
7. **Wölfel R, Cormon VM, Guggemos W**, et al. Nature 2020;581:465–469.
8. Lee DS, Kim JW. Endoscopy 2021;53:207–208.

*Authors share co-first authorship. §Authors share co-senior authorship.

Author names in bold designate shared co-first authorship.

Supplementary Methods

The method is based on several important facts regarding the scattering of light by spherical droplets in the close to forward direction. Firstly, such scattering can be accurately described using an exact solution for the scattering of electromagnetic plane waves by a dielectric spherical scatterer introduced by Mie.[4] The Mie solution shows that for water droplets with diameters of ≥ 5 μm in air, there is a significant scattering peak in the close to forward direction, which could be strong enough to be observed even for a fast-flying droplet.

Secondly, the scattering patterns from droplets of different sizes are quite unique. This allows accurate characterization of the droplet sizes, with sphere size extracted from the angular frequency of intensity oscillations. This is illustrated in Supplementary Figure 1A, where the scattering pattern for 2 droplets (diameters of 20 μm and 50 μm) are plotted, with the larger droplet clearly exhibiting more intensity oscillations. The Mie solution-based relationship for the angular increment between successive peaks in the scattering pattern vs the inverse diameter of droplets in the 20- to 120-μm range is illustrated in Supplementary Figure 1B. Supplementary Figure 1C shows the averaged scattering pattern (*red dotted line*) for the droplet shown in Figure 1G, which is compared with the best fit theoretical curve (*blue solid line*). This theoretical curve was produced using Mie scattering theory for a 41-μm water droplet in air, with a constant background term added. The system was optimized to measure droplets larger than aerosols, because viral load is proportional to the droplet volume. For example, a 50-μm droplet has a volume 1000-times larger than a 5-μm aerosol and, therefore, carries an approximately 1000-times higher viral load.

MATLAB code (MathWorks) was written to automatically detect frames containing scattering patterns. These frames of interest were then analyzed with an algorithm to detect only frames where a droplet, and not particles, crossed the beam. For frames that contained droplet scattering, a polar transform was applied, and the oscillations were averaged azimuthally. Peak detection was then used to determine the number of cycles/mm for the scattering pattern. Theoretical analysis was performed to obtain the expected cycles/mm for scattering patterns produced by water droplets of different sizes when measured with our system. This analysis was compared with the experimental values to return the droplet size. The system and analysis code were validated by measuring the scattering pattern of polystyrene beads (diameters of 45 μm and 90 μm) suspended in water. The returned sizes were within the manufacturer's tolerance.

We were unable to find studies that reported the distribution of size or quantity of droplets produced during gastrointestinal endoscopy. As a result, a sample size calculation was not possible, and we therefore chose to enroll 10 patients undergoing upper endoscopy and 10 patients undergoing colonoscopy into our study. Data are presented as mean ± standard error in the figures. Statistical analysis was completed using GraphPad Prism 8 software (GraphPad Software).

Anderson-Darling tests and D'Agostino-Pearson tests were used to determine whether the data met the assumption of normality. When comparing multiple groups, we used analysis of variance with Dunnett's multiple comparisons test if data were normally distributed, and the Kruskal-Wallis test with Dunnett's multiple comparisons test was used if the data were not normally distributed. When 2 groups were compared, 2-tailed Mann-Whitney U test was used if data were not normally distributed. P values <.05 were considered statistically significant. Specific analysis is detailed in the figure legends, and no data were excluded in our analysis. In the figures, standard designations of significance are given: $*P < .05$; $**P < .01$; $***P < .001$; $****P < .0001$. Specific analysis is detailed in the figure legends and no data were excluded in our analysis.
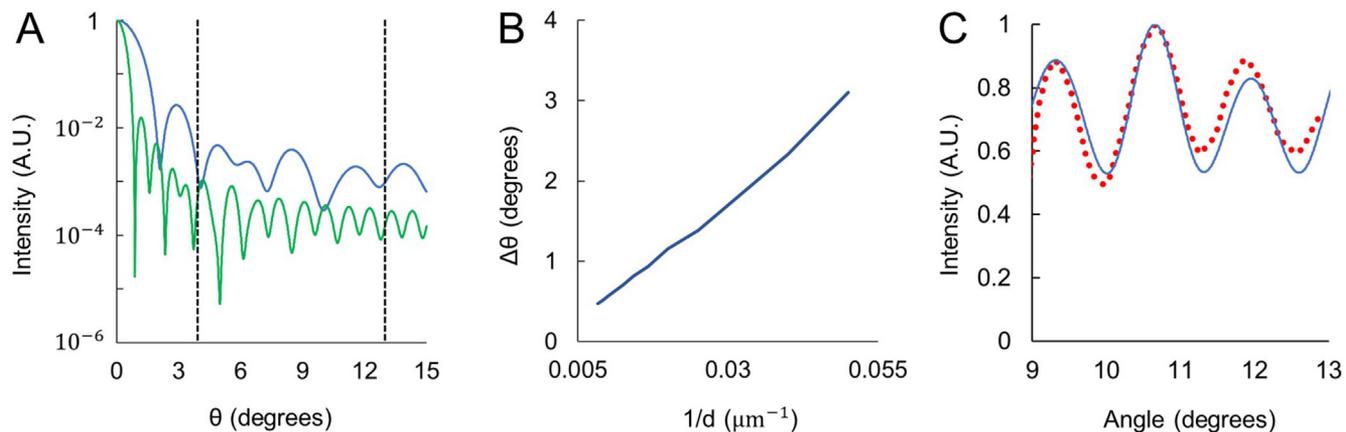
Supplementary Figure 1. (*A*) Mie based scattering intensity distributions for a 20 μm (*blue*) and 50 μm (*green*) diameter droplet. More oscillations are clearly observed for the 50-μm droplet. The *black dashed lines* illustrate the experimentally measured region (between 4° and 13°). A.U., arbitrary units. (*B*) Angular increments between successive extrema of the light scattering distribution calculated using Mie theory. (*C*) An example droplet scattering pattern after an averaged polar transform (*red dotted line*) and best fit theoretical curve (*blue line*) calculated from a 41-μm diameter droplet.

Supplementary Table 1. Patient and Room Information for 10 Upper Endoscopies and 10 Colonoscopies

Patient No.	Proc type	θ, ° Min	Max	L, cm Min	Max	Humidity, % RH	Temp, C°	POM mask	Pre-Proc, min	Proc, min	Post-Proc, min
1	Colon	0	10	60	90	44	21.5	n/a	8.5	19.2	8.0
2	Colon	0	10	60	75	45	21.5	n/a	7.1	18.7	10.1
3	EGD	5	15	30	45	45	22.0	No	6.1	10.6	9.2
4	EGD	0	30	30	45	45	22.0	No	12.5	13.8	10.6
5	Colon	0	10	60	90	45	22.0	n/a	5.5	25.8	12.8
6	EGD	0	15	30	50	43	21.5	No	13.3	9.2	8.2
7	EGD	0	10	20	45	43	21.5	No	7.7	4.5	8.5
8	Colon	0	10	45	90	44	21.5	n/a	12.0	21.3	12.6
9	Colon	0	10	60	90	43	21.5	n/a	6.5	23.7	10.6
10	Colon	0	10	60	90	43	21.5	n/a	8.0	32.7	15.3
11	EGD	0	10	30	45	36	20.5	Yes	4.8	6.6	9.3
12	EGD	5	15	30	45	34	20.5	Yes	8.0	10.3	5.5
13	Colon	−5	5	60	90	32	21.0	n/a	7.1	18.8	12.0
14	EGD	5	35	30	45	30	21.5	Yes	7.6	5.4	1.5
15	EGD	0	25	30	45	29	21.5	Yes	7.4	8.4	7.6
16	Colon	−5	5	45	90	28	21.5	n/a	4.0	19.0	18.5
17	EGD	0	25	30	45	28	21.5	Yes	9.9	7.6	3.5
18	EGD	0	10	30	45	28	22.0	Yes	6.6	3.2	5.7
19	Colon	−10	0	60	90	29	22.0	n/a	3.4	15.5	10.2
20	Colon	−10	0	45	60	29	21.5	n/a	7.3	15.7	5.8

NOTE. During some esophagogastroduodenoscopy (EGD) procedures (Proc), the patient wore a procedural oxygen mask (POM). Angle (θ) and distance (L) notation are illustrated in Figure 1E. Angles are defined relative to the oral axis for upper endoscopies, with positive angles toward the nose of the patient. Angles are defined relative to the anal canal axis for colonoscopies, with positive angles towards the patient front. The mean ± standard error duration of the upper endoscopies and colonoscopies was 7.9 ± 1.0 minutes and 21.0 ± 1.6 minutes, respectively. The mean duration of the preprocedure (Pre-Proc) control and postprocedure control (Post-Proc) was 7.7 ± 0.6 minutes and 9.3 ± 0.9 minutes, respectively.
Max, maximum; Min, minimum; n/a, not applicable; RH, relative humidity.